Crystal Growth and Dielectric Study of the Niobate Series $K_3Sr_2RNb_{10}O_{30}$ (R = Lanthanide) of Tungsten Bronze Structure

A. Lahmar[1], S. Ganschow[2], J. Doerschel[2], K. Tsuzuku[3,4], M. Couzi[3] and B. Elouadi[1]*

[1]Laboratoire d'Elaboration, Analyse Chimique et Ingenierie des Materiaux (LEACIM), Universite de La Rochelle, avenue Michel Crepeau, 17042 La Rochelle Cedex 01, France

[2]Institut fur Kristallzuchtung, Max Born-Stor. 2, D-12489 Berlin, Germany

[3]Groupe de Spectroscopie Moleculaire (GSM) Institut des Sciences Moleculaires (ISM) UMR 5255- CNRS, Universite Bordeaux1, cours de la Liberation, 33405 Talence, France

[4]R&D Materials Departement, General R&D Laboratorises, Taiyo Yuden R&D Center 5607-2 Nakamuroda – Machi Gunma – Gun Gunma 370-3347, Japan

Abstract

Fibre single crystals of $K_3Sr_2RNb_{10}O_{30}$ (R = La, Nd, Eu, Gd, Sm) have been successfully grown using the μ-pulling down method. Single crystal X-ray diffraction technique has confirmed that all isolated compounds crystallize with the tetragonal tungsten bronze structure. The elemental analyses of Nd- and Eu-crystals using EDX has evidenced the presence of some inclusions corresponding to the composition KNb_3O_8. The presence of such compound in the matrix of the grown fibres could be interpreted as a revelation of the quaternary equilibrium involved during the crystal growth. Dielectric and Raman investigations within a wide temperature range [–150°C; 400°C], tend to confirm the existence of the same thermal anomalies. Although these anomalies are found at almost the same temperatures, the nature and the mechanisms of the so-revealed phase transitions are not yet totally evidenced.

Introduction

Niobate compounds crystallizing with the tetragonal tungsten bronze structural type (TTB) have been investigated due to their potential applications of importance in many electronic and electro-optical domains: SAW devices [1], electro optics [2], dielectric and piezoelectric devices [3-6], *etc*. The rare earth niobate compounds with the general formula $K_3Sr_2RNb_{10}O_{30}$ (R = La, Nd, Sm, Eu, Gd) have been more particularly investigated with regard from the one hand, to the technological interest (lasers, phosphors, etc.) for the determination of the spectroscopic characteristics of the luminescence of lanthanide ions (Ln^{3+}) in such class of materials and from the other hand, to the possibility offered by the use of rare earth ions as local probes in order to obtain key structural information not often accessible using X-ray diffraction techniques. In the present article, we report the preliminary results of our work on the crystal fibres grown by the μ-pulling down method and analysed using various techniques such as: single crystal and powder XRD, energy dispersive spectroscopy (EDS), High and low temperature dielectric and Raman measurements. One of our purposes was the approach of the nature and the mechanisms of the phase transitions related to the series of materials $K_3Sr_2RNb_{10}O_{30}$ (R = Rare Erath), isolated with the tetragonal tungsten bronze structure.

Experimental

The crystal fibres of the title compounds were grown using the μ-polling down technique [7]. As schematically represented in Fig. 1, this technique consists here to melt a powdered sample of the desired composition initially isolated as a pure phase, in a platinum crucible terminated by a micro-nozzle at

*corresponding authors. E-mail: belouadi@univ-lr.fr

Printed in Kazakhstan

the bottom. The melted material is then passed through the micro-nozzle to form a rod-shaped micro-single-crystal with a cross-section and a modulated diameter of about 1 mm. The position of the liquid-solid interface and the crystal diameter are controlled by adjustments of the pulling rate and heating power supplied to the crucible.

In other variants of the experimental set-up [12] which has not been used here, the resulting fibres could be sintered (after crystallisation), on cooling with a rate that is monitored using a second furnace (after growth heater) located below the micro-nozzle as shown on Fig. 1.

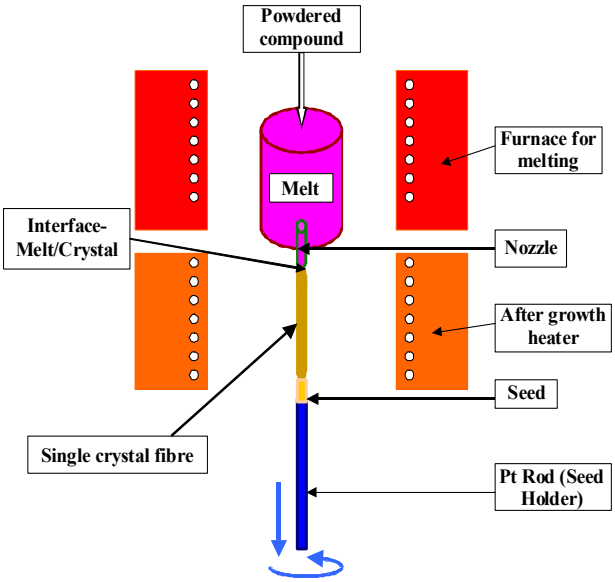

Fig. 1. Experimental diagram for the crystal growth by the μ-pulling down method.

Results and Discussions

Crystal Analysis and Phase Equilibrium Diagrams

Figure 2 represents a typical example of crystal fibres, grown in the course of the present study by the μ-polling down method. The isolated crystal fibres were of sufficiently big size and the quality that allowed their use both for the structure resolution and the investigation of some physical measurements like luminescence of rare earth ions for example [8].

As shown in Figure 3, it is also worth to notice that the series $K_3Sr_2RNb_{10}O_{30}$ (R = La, Nd, Eu, Gd, Sm) is part of the ternary diagram $KNbO_3$–$SrNb_2O_6$–RNb_3O_9 and particularly its line $KSr_2Nb_5O_{15}$–$K_2RNb_5O_{15}$

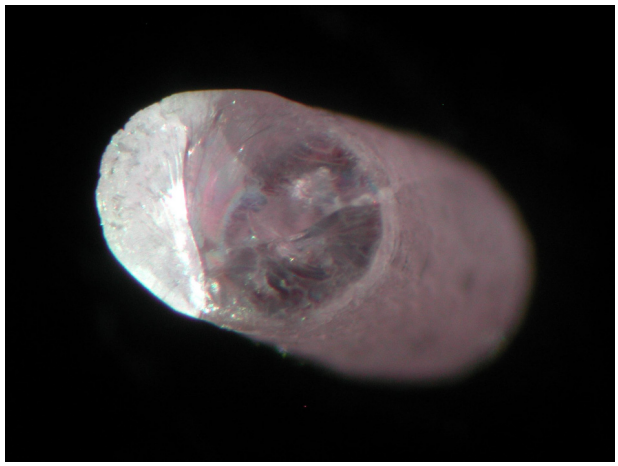

Fig. 2. Morphology of a typical single crystal fibre of $K_3Sr_2NdNb_{10}O_{30}$ grown by the μ-pulling down technique.

Nb_5O_{15}. As a matter of fact, the title compounds can result from the equilibrium given by one of the following equations (Eqs. 1-3):

$$KNbO_3 + SrNb_2O_6 + RNb_3O_9 \leftrightarrows K_3Sr_2RNb_{10}O_{30} \quad (1)$$

$$KSr_2Nb_5O_{15} + K_2RNb_5O_{15} \leftrightarrows K_3Sr_2RNb_{10}O_{30} \quad (2)$$

$$K_{4-x}Sr_{2x}R_{1-x}Nb_{10}O_{30} \quad (3)$$

Indeed, the series $K_3Sr_2RNb_{10}O_{30}$ (R = La, Nd, Eu, Gd, Sm) correspond to $x = 0.5$ in the formula (Eq. 3) of the solid solution having its two limits, $KSr_2Nb_5O_{15}$ and $K_2RNb_5O_{15}$, crystallising with the TTB structure [9-12]. It is therefore expected that all the compositions of this line will adopt the tetragonal tungsten bronze structural type (Fig. 3).

The elemental analysis of the fibres was performed over all their length by EDX microprobe technique. As can be seen from the results given in Table 1, in

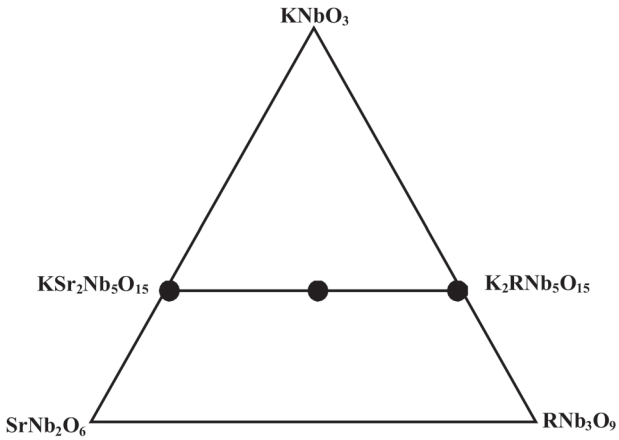

Fig. 3. Location of the phase $K_3Sr_2RNb_{10}O_{30}$ within the ternary system $KNbO_3$–$SrNb_2O_6$–RNb_3O_9 with R = rare earth.

addition to the main phase $K_3Sr_2NdNb_{10}O_{30}$, some trace impurities have been detected. These impurities correspond to the compositions KNb_3O_8:doped (Sr, Nd). However, in the case of $K_3Sr_2EuNb_{10}O_{30}$ fibres (Table 2), the second phase inclusion corresponds to the same compound KNb_3O_8, but the latter seems to be rare earth free. In the present elemental analysis, it worth to mention that all results are given in at percentage (at. %) and the oxygen ratio was determined considering a total stoichiometry for all oxides, with the maximum oxidation degree for all cations. The appearance of the second phase, KNb_3O_8, in the process of the crystal growth can be seen as the revelation of a more complex equilibrium during the growth process. As a matter of fact, KNb_3O_8 belongs to the binary system K_2O–Nb_2O_5 and does not appear in the ternary diagram given in Fig. 3. Therefore, from these analysis, it is expected that the phase equilibrium during the crystal growth will involve the phase compatibility in the quaternary system K_2O–SrO–R_2O_3–Nb_2O_5 and not only the basic compositions of the ternary diagram $KNbO_3$–$SrNb_2O_6$–RNb_3O_9. The latter ternary representation is given because it evidences the chemical correlation along the line represented by the formula of Eq. 3, for $x = 0$, $x = S$ and $x = 1$.

Dielectric Measurements of $K_3Sr_2RNb_{10}O_{30}$ (R = La, Nd, Eu, Gd, Sm,Yb)

Dielectric measurements were performed at two different frequencies: 1 MHz and 1 kHz. Contact electrodes were made by deposited silver paste on both faces of the sample disks. Two different chambers were used to obtain whole data. One was used for measurements at temperatures higher than 20°C, and the other was for the range 70-290 K. Figure 4 represents the thermal variations of the capacitance

Table 1
EDX element analysis of Nd-single crystal fibre grown by μ-pulling down method

Sample N°	K	Sr	Nb	Nd	O
Matrix-1	5.90	4.81	21.40	2.65	65.24
Matrix-2	5.81	4.94	21.39	2.61	65.25
Matrix-3	4.87	5.05	21.64	2.74	65.70
Matrix-4	5.53	4.85	21.58	2.59	65.45
Matrix-5	5.47	4.73	21.64	2.64	65.52
Average	5.52	4.9	21.53	2.65	65.43
Deduced formula $K_{2.53}Sr_{2.24}Nd_{1.22}Nb_{9.87}O_{30}$					
Theorical values	6.52	4.35	21.74	2.17	65.22
Retained Experimental formula $K_3Sr_2NdNb_{10}O_{30}$					
Foreign-1	8.46	0.69	24.24	0.13	66.18
Foreign-2	7.40	1.14	24.32	0.21	66.54
Foreign-3	7.84	0.90	24.28	0.21	66.39
Foreign-4	7.73	0.96	24.31	0.22	66.44
Foreign-5	8.09	0.62	24.37	0.18	66.38
Foreign-6	6.84	2.04	24.12	0.15	66.50
Average	7.73	1.1	24	0.18	66.4
Deduced formula $Sr_{0.132}Nd_{0.02}K_{0.93}Nb_{2.89}O_{7.97}$					
Theatrical values	8.33	-	25	-	66.67
Retained experimental formula KNb_3O_8 : doped (Sr, Nd)					

Table 2
EDX element analysis of the Eu-single crystal fibres grown by the μ-pulling down method

Sample N°	K	Sr	Nb	Eu	O
Matrix-1	5.73	5.53	21.47	2.09	65.19
Matrix-2	5.79	5.08	21.46	2.41	65.25
Matrix-3	5. 76	5.20	21.55	2.22	65.28
Matrix-4	5.58	5.18	21.55	2.33	65.35
Matrix-5	5.39	5.28	21.62	2.27	65.44
Matrix-6	5.68	4.87	21.60	2.46	65.39
Matrix-7	5.44	5.41	21.53	2.27	65.36
Average	5.62	5.22	21.54	2.29	65.32
Deduced formula $K_{2.58}Sr_{2.40}Eu_{1.01}Nb_{9.89}O_{30}$					
Theorical values	6.52	4.35	21.70	2.17	65.22
Retained Experimental formula $K_3Sr_2EuNb_{10}O_{30}$					
Foreign-1	10.73	0	23.97	0	65.30
Foreign-2	7.24	2.07	24.28	0	66.41
Foreign-3	7.85	1.25	24.49	0	66.41
Foreign-4	7.69	1.18	24.60	0	66.53
Foreign-5	7.39	1.65	24.46	0	66.50
Foreign-6	12.35	0	23.28	0	64.38
Average	8.88	1.03	24.18	0	65.92
Deduced formula $K_{1.08}Sr_{0.12}Nb_{2.93}O_8$					
Theorical values	8.33	-	25	-	66.67
Retained Experimental formula KNb_3O_8					

(at 1 MHz and 1 kHz) for different rare earth compounds. As can be seen from these figures, the dielectric plots show peaks which could reveal some phase transitions. The nature of such lattice change is not yet clearly identified. However, the values of the peak temperatures show no significant change with frequency, although the frequency measurement has been varied from 1 kHz to 1 MHz. This could be interpreted as a revelation for a non relaxor character of the corresponding transition.

Indeed it is also worth to mention the narrow and relatively strong peaks observed close to 273 K for only one frequency (1 kHz). Such peak could be attributed to either a phase transition or to water desorption from the surface of the investigated ceramics on heating! Another origin could be the melting of the deposited ice on the ceramics which implicates more mobile hydrogen bonds than in solid water. More experimental evidences are needed before to decide of the nature of the dielectric peak recorded in the vicinity of 0°C, for the niobate ceramics, as shown in Fig. 4. Adsorpded water at the surface of our ceramics could be attributed to the moisture of environmental air.

Thermal Raman Spectroscopy of $K_3Sr_2RNb_{10}O_{30}$ (R = Nd) and Evidence of Phase Transitions

Figure 5 represents the thermal variation of the Raman spectra recorded for $K_3Sr_2NdNb_{10}O_{30}$, within the temperature range 120-673 K. The peaks are rather broad, alike in glasses or in highly disordered structures. In addition, the temperature does not seem to have any brutal effect on the progressive change of the obtained Raman spectra. As discussed elsewhere [8], some vibration modes ν_2 and ν_3, tend to

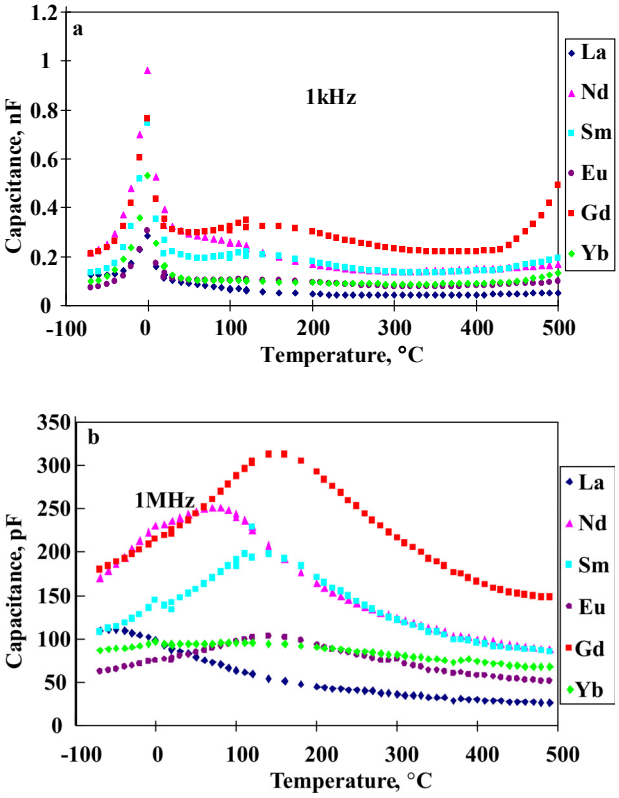

Fig. 4. Thermal variation of capacitance at 1 kHz (a) and 1 MHz(b) of the ceramics $K_3Sr_2RNb_{10}O_{30}$ (R = La, Nd, Eu, Gd, Sm and Yb).

disappear at almost the same temperature of the dielectric peaks shown in Fig. 4. However, the raw Raman experimental data tend to show a rather smooth thermal evolution. Indeed, the analysis of the change of Raman spectra versus temperature seems to indicate some slight variation in the intensity of the vibration modes having their frequencies ranging around 900-1300 cm^{-1}. Such bands tend to disappear for temperatures higher than 0°C. In order to get a better insight into the thermal change of the Raman spectra, recorded in the present study, we carried out a de-convolution of some vibration bands as shown in Fig. 6. As a matter of fact, this figure represents a typical example obtained for the main line (ν_4) using a Gaussian function. As can be evidenced from Figures 7 and 8, some parameters taken from the Raman data, show clear anomalies on their plots versus temperature. These anomalies have been considered as a revelation of a certain type of phase transition. For instance, the thermal variation of the peak position of the line $(\nu_4)_1$ of this mode, is given in Fig. 7. As can be seen in this figure, the plot shows a rather clear anomaly at 0°C in the same temperature range where a maximum of dielectric constants was observed (Fig.

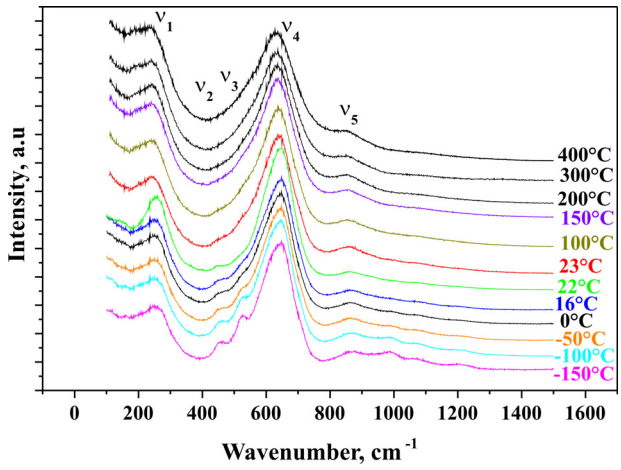

Fig. 5. Thermal variation of Raman spectra of $K_3Sr_2Nd-Nb_{10}O_{30}$.

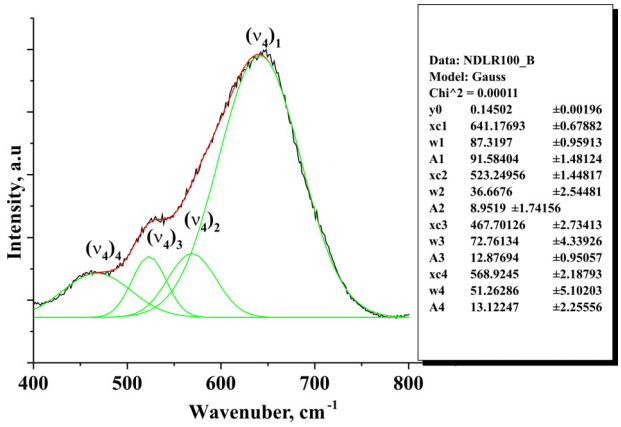

Fig. 6. Typical example of resolved spectra of the strong Raman mode line (ν_4) in $K_3Sr_2NdNb_{10}O_{30}$.

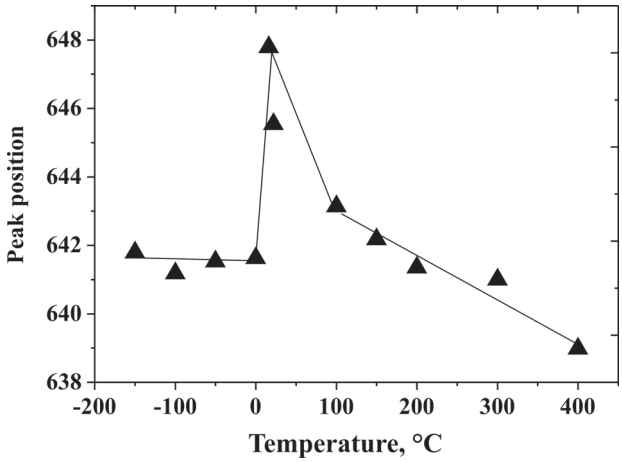

Fig. 7. Thermal variation of the peak position (cm^{-1}) of the main line $(\nu_4)_1$.

4). In order to tempt to give more evidence for the existence of other anomalies and therefore reveal the

presence of phase transitions in the title series of compounds, we have represented the thermal plots of the intensity ratios: $I(\nu_4)_3/I(\nu_4)_1$, $I(\nu_4)_3/I(\nu_4)_4$ and $I(\nu_4)_4/I(\nu_4)_1$. All recorded graphs in Figures 7 and 8, tend to give evidences for clear phase transitions at approximately the same temperatures determined from dielectric measurements. In addition to the broad Raman lines, such behaviour was attributed here to the existence of a kind of order-disorder of transitions whose nature and mechanisms are yet to be clarified. Indeed, it seems that there is a convergence versus temperature of the Raman and dielectric behaviour of all investigated samples. This is very satisfying for such considerations. However, there is still a need for more fine structural data in order to identify the atomic origin of the revealed phase transitions.

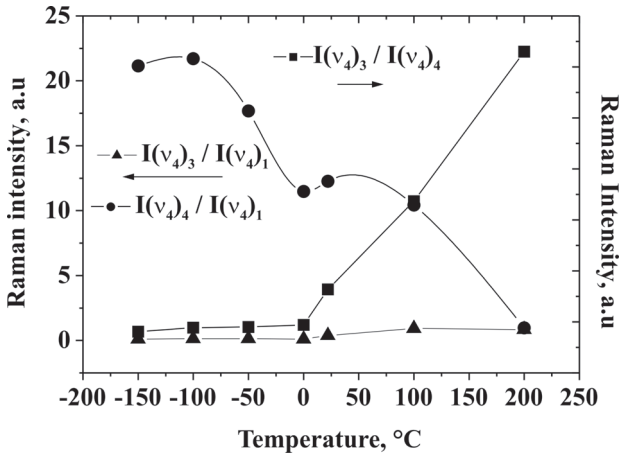

Fig. 8. Thermal variation of the Raman intensity ratios $I(\nu_4)_3/I(\nu_4)_1$, $I(\nu_4)_3/I(\nu_4)_4$ and $I(\nu_4)_4/I(\nu_4)_1$ for the neodymium compound $K_3Sr_2NdNb_{10}O_{30}$.

Conclusions

Fibre single crystals of $K_3Sr_2RNb_{10}O_{30}$ (R =La, Nd, Eu, Gd, Sm) have been successfully grown using the μ-pulling down technique. The elemental analyses of Nd- and Eu- crystals by EDX evidenced the presence of impurities corresponding to the composition KNb_3O_8. The presence of such compound in the matrix of the grown fibres could be interpreted as a revelation of the equilibriums involved during the crystal growth.

Dielectric and Raman investigations with temperature tend to confirm the existence of the same thermal anomalies in this important series of rare earth mixed niobate oxides. Although the peaks are found at almost the same temperatures, the nature of the phase transitions they evidence is not yet totally explained. A type of order-disorder mechanism has been considered.

References

1. E.L. Ventiurini, E.G. Spencer and A.A. Ballman; J. Appl. Phys., 40, 1622 (1969).
2. P.V. Nenzo, E.G. Sencer and A.A. Balman; J. Appl. Phys. Lett., 11, 23 (1971).
3. M.E. Lines, and A.M. Glass; "Principles and Applications of Ferroelectrics and Related Materials", Clarendon Press, Oxford (1979).
4. B. Elouadi, Thиse de Doctorat d'Etat, Universitй de Bordeaux 1, France (1976).
5. V.S. Filip'ev, Y.A.E. Cherner, Z.V. Bondarenko and E.G. Fesenko; Sov. Phys. Solid State, 28(5), 753 (1986).
6. B.N. Savenka, B. Sangaa and F. Proket; Ferroelectrics, 107, 207 (1990).
7. D.H. Yoon, H. Yamamura and T. Orito; J. Crystal Growth, 110, 669 (1991).
8. S. Lanfredi, C.X. Cardoso and M.A.L. Nobre; Mat. Sci. Engineering, B112, 139 (2004).
9. E.A. Giess, G. Burns, D.F. O'Kane and A.W. Smith; Appl. Phys. Lett., 11, 233 (1967).
10. B.A. Scott, E.A. Giess, G. Burns and D.F. O'Kane; Mat. Res. Bull., 3, 831 (1968).
11. R.R. Neurgaonkar, J.G. Nelson and J.R. Oliver; Mat. Res. Bull., 25, 959 (1990).
12. A. Lahmar; Thиse de Doctorat, University Mohammad-5, Faculty of Science, Rabat-Morocco (2007).

Received 12 July 2008.